Formation of the Surface NO during N_2O Interaction at Low Temperature with Iron-Containing ZSM-5

Dmitri A. Bulushev, Albert Renken, and Lioubov Kiwi-Minsker*

Ecole Polytechnique Fédérale de Lausanne, LGRC-EPFL, CH-1015 Lausanne, Switzerland

Received: September 8, 2005; In Final Form: November 8, 2005

Interaction of N_2O at low temperatures (473−603 K) with Fe−ZSM-5 zeolites (Fe, 0.01−2.1 wt %) activated by steaming and/or thermal treatment in He at 1323 K was studied by the transient response method and temperature-programmed desorption (TPD). Diffuse reflectance infrared fourier transform spectroscopy (DRIFTS) of NO adsorbed at room temperature as a probe molecule indicated heterogeneity of surface Fe(II) sites. The most intensive bands were found at 1878 and 1891 cm^{-1}, characteristic of two types mononitrosyl species assigned to Fe^{2+}(NO) involved in bi- and oligonuclear species. Fast loading of atomic oxygen from N_2O on the surface and slower formation of adsorbed NO species were observed. The initial rate of adsorbed NO formation was linearly dependent on the concentration of active Fe sites assigned to bi- and oligonuclear species, evolving oxygen in the TPD at around 630−670 K. The maximal coverage of a zeolite surface by NO was estimated from the TPD of NO at ∼700 K. This allowed the simulation of the dynamics of the adsorbed NO formation at 523 K, which was consistent with the experiments. The adsorbed NO facilitated the atomic oxygen recombination/desorption, the rate determining step during N_2O decomposition to O_2 and N_2, taking place at temperatures ≥563 K.

1. Introduction

N_2O decomposition to N_2 and O_2 over Fe−ZSM-5 catalysts is known to take place at temperatures higher than 573 K. This reaction involves Fe-containing sites, $(\ )_{Fe}$, and takes place via atomic oxygen loading from N_2O:

$$N_2O + (\ )_{Fe} \rightarrow N_2 + (O)_{Fe} \qquad (1)$$

Recently, the evidence was presented that adsorbed NO and NO_x species are also formed during N_2O interaction with Fe−ZSM-5 zeolites.[1−3] Thus, Grubert et al.[3] by "in situ" FTIRS observed the formation of adsorbed NO on Fe(II) sites of Fe−ZSM-5 and Fe−MCM-41 during an interaction with N_2O at room temperature. El-Malki et al.[2,4] also observed at 473 K surface nitro- and nitrate groups formation from N_2O similar to those obtained by direct interaction of a NO/O_2 mixture with the catalysts prepared by sublimation of $FeCl_3$ onto ZSM-5. The temperature-programmed desorption (TPD) from the catalysts exposed to N_2O gave an NO peak with a maximum at around 653 K.[2] Mauvezin at el.[5] observed an evolution of NO at around 600 K during the temperature-programmed reduction of Fe−β zeolites with hydrogen after their oxidation in N_2O. Novakova et al.[6] observed the formation of NO and NO_2 in TPD performed after N_2O decomposition over Fe-ferrierite at 553 K. In line with all these results, we found[1] that adsorbed NO species are slowly accumulated on the surface of Fe−ZSM-5 catalyst with low iron content and strongly affect the dynamics of N_2O decomposition, leading to an increase of the reaction rate with time.

Reaction 2 is often considered as responsible for the formation of NO/NO_x surface species:

$$2N_2O \rightarrow 2NO + N_2 \qquad (2)$$

The active sites are related to iron, but their nature is still not clear because of the complexity of the state of iron in zeolites. Framework Fe(III) species, surface extraframework isolated bi- and oligonuclear Fe(II) sites and bulk Fe_2O_3/Fe_3O_4 nanoparticles have been reported to be present in the samples, depending on iron content and zeolite pretreatment.

Fe-containing zeolites are not unique for the NO formation from N_2O. Evolution of gaseous NO/NO_2 was observed during the TPD after the contact of N_2O with Cu−ZSM-5 catalysts at 598 K. However, with Cu−mordenite and Cu−Y zeolites, this was not the case.[7] Traces of gaseous NO/NO_2 were also detected during the N_2O decomposition to O_2 and N_2 over Cu−ZSM-5 zeolites.[7,8]

The formation of adsorbed NO from N_2O attracts much attention because this species promotes the N_2O decomposition to O_2 and N_2 over Fe−ZSM-5 catalysts.[1,9−16] The decomposition involves the formation of surface atomic oxygen from N_2O (reaction 1), followed by its recombination with desorption as the rate-determining step

$$2(O)_{Fe} \rightarrow O_2 + 2(\ )_{Fe} \qquad (3)$$

This step is facilitated by adsorbed NO, accelerating the overall reaction:[1,11]

$$2(O)_{Fe} + [NO] \rightarrow O_2 + [NO] + 2(\ )_{Fe} \qquad (3a)$$

Recently, we proposed a kinetic model for N_2O decomposition by taking into account the formation of adsorbed NO promoting the N_2O decomposition to O_2 and N_2.[17] The present work aims to clarify the regularities of the adsorbed NO formation on Fe−ZSM-5 zeolites from N_2O. The surface iron sites in Fe−ZSM-5 catalysts are characterized by the adsorption of NO as a probe molecule at room temperature controlled by DRIFTS. The total amount of surface Fe(II) sites is determined by the transient response method at 523 K. The amount of Fe-

* To whom correspondence should be addressed. E-mail: lioubov.kiwi-minsker@epfl.ch.

10.1021/jp055067t CCC: $33.50
Published on Web 12/08/2005

TABLE 1: Main Characteristics of the Studied Fe-ZSM-5 Catalysts

catalyst	Fe loading wt %	Si/Al ratio	steaming	time of activation in He at 1323 K, h	iron active sites $\times 10^{-18}$, sites g^{-1}	
					C_{Fe}^{Σ}	C_{Fe}^{TPD}
Activated by Thermal Treatment in He at 1323 K						
$ZSM\text{-}5_{110}$	0.011	42	-	1	0.062	0
$ZSM\text{-}5_{110}$	0.011	42	-	20	0.021	0
$ZSM\text{-}5_{150}$	0.015	25	-	1	0.55	0.34
$ZSM\text{-}5_{200}$	0.02	42	+	20	2	1.2
$ZSM\text{-}5_{300}$	0.03	47	+	20	0.83	0.64
$ZSM\text{-}5_{350}$	0.035	42	-	1	2.8	1.9
$ZSM\text{-}5_{350}$	0.035	42	+	1	3.0	2
$ZSM\text{-}5_{470}$	0.047	42	-	1	2.1	1.4
$ZSM\text{-}5_{5500}$	0.55	25	-	1	3.9	2.6
$ZSM\text{-}5_{5800}$	0.58	25	+	1	11	10.3
$ZSM\text{-}5_{5800}$	0.58	25	+	4	8.4	7
$ZSM\text{-}5_{5800}$	0.58	25	+	8	7.2	4.8
$ZSM\text{-}5_{5800}$	0.58	25	+	11	6.3	4.4
$2.1\%Fe{-}ZSM\text{-}5_{150}$	2.1	25	-	1	24	10
Activated by Steaming and Thermal Treatment in He at 823 K						
$ZSM\text{-}5_{350}$	0.035	42	+	0	0.8	0.13
$ZSM\text{-}5_{5800}$	0.58	25	+	0	7.3	2.4
$2.1\%Fe{-}ZSM\text{-}5_{150}$	2.1	25	+	0	28.9	11.6

(II) sites involved in O_2 formation via reaction 3 are measured by the TPD of oxygen evolved at 620−670 K.[18,19]

2. Experimental Section

2.1. Catalyst Preparation. Both commercially available and homemade ZSM-5 zeolites were used in the present study (Table 1). The industrial Zeocat PZ-2/50H (Si/Al = 25, H form) as extrudates ($ZSM\text{-}5_{5500}$) and powder ($ZSM\text{-}5_{150}$) were provided by Zeochem AG (Uetikon, Switzerland). The powder contained 150 ppm of Fe as an impurity, and the extrudates were found to contain 5500 ppm of iron due to a binder used for pelletizing. The isomorphously substituted ZSM-5 with Si/Al = 42 or 47 were synthesized via the hydrothermal route. Typically, tetraethyl orthosilicate (TEOS, Fluka, 98%) was added to an aqueous solution of tetrapropylammonium hydroxide (TPAOH, Fluka, 20% in water) used as a template, $NaAlO_2$ (Riedel-de Haën, Na_2O 40−45%, Al_2O_3 50−56%), and $Fe(NO_3)_3{\cdot}9H_2O$ (Fluka, 98%). The molar ratios between components were TEOS/TPAOH/$NaAlO_2$/H_2O = 0.8:0.1:0.016−0.032:33 and Si/Fe = 160−3200. The mixture was stirred for 3 h at room temperature, and the final clear gel was transferred to a stainless steel autoclave lined with Teflon and kept in an oven at 450 K for 2 days. The product was filtered, washed with deionized water, and calcined in air at 823 K for 12 h. The zeolite was then converted into the H form by an exchange with a NH_4NO_3 aqueous solution (0.5 M) and subsequent calcination at 823 K for 3 h. A postsynthesis iron deposition was performed with the $ZSM\text{-}5_{150}$ by the adsorption from an $Fe(CH_3COO)_3$ aqueous solution (0.01 M) (for $2.1\%Fe{-}ZSM\text{-}5_{150}$). This sample had an intensively brown color, indicating Fe_2O_3 formation.

The catalysts were activated by steaming (H_2O partial pressure of 0.3 bar, He flow rate 50 mL/min) at 823 K for 4 h and/or by treatment at 1323 K in a He flow (50 mL/min) for 1−20 h.[19] The main characteristics of the samples are shown in Table 1.

To prepare an Fe_2O_3/Al_2O_3 sample, iron oxide was deposited on alumina by incipient wetness impregnation with 2.2 M $Fe(NO_3)_3{\cdot}9H_2O$ solution, followed by drying in air at room temperature and calcination at 823 K for 4 h.

2.2. Catalyst Characterization. The chemical composition of the catalysts was determined by atomic absorption spectroscopy (AAS) via a Shimadzu AA-6650 spectrometer. The samples were dissolved in hot aqua regia containing HF.

Catalysts were characterized by "in situ" DRIFTS of adsorbed NO at 303 K. A Perkin-Elmer 2000 FTIR spectrometer with an MCT detector was used. The catalyst (~0.015 g) ground in an agate mortar was placed into a SpectraTech 003−102 DRIFTS cell with CaF_2 windows in a setup described earlier.[20] The setup allowed quick switching between two flows, one with pure Ar, another containing 0.5 vol % of NO in Ar. The flow rate was equal to 20 mL (STP)/min. The spectra of the nitrosyl region (1740−1940 cm^{-1}) were almost identical during 2−6 min in NO. After 6 min, the flow passing through the catalyst was switched back to Ar. The DRIFT spectra obtained by averaging of 32 scans with a resolution of 4 cm-1 were taken every 0.5 min. Before every run, the activated catalysts were pretreated in the cell in Ar at 823 K for 60 min. A single beam spectrum of the catalyst before introduction of NO into the cell at the interaction temperature was taken as a background. The contribution of the gaseous NO to the spectra was negligible, as shown by measuring the spectra of the mixture containing 0.5 vol % NO over KBr.

2.3. Transient Response and TPD Measurements. Transient response and TPD experiments were performed in a Micromeritics AutoChem 2910 analyzer. A ThermoStar 200 (Pfeiffer Vacuum) quadrupole mass spectrometer was used for gas analysis. Calibrations were carried out with gas mixtures of known compositions. The following peaks were controlled simultaneously by the mass spectrometer 4 (He), 18 (H_2O), 28 (N_2, N_2O), 30 (NO, N_2O), 32 (O_2), 40 (Ar), 44 (N_2O), and 46 (NO_2) *m*/*e*. The lines in the setup as well as a fused silica capillary connected to the mass spectrometer were heated to 383 K. Sometimes, a NO_x detector (EcoPhysics CLD 822) with a sensitivity of ≥10 ppm of NO_x was used to identify the nitrogen oxides at the reactor outlet.

The amount of a catalyst placed in a quartz plug-flow reactor was equal to 0.5−1.0 g. Before every run, the activated catalysts were pretreated in He (50 mL/min) at 823 or 1323 K for 1 h (Table 1), then cooled to the studied temperature.

In the transient response experiments, normally a 2 vol % N_2O/2 vol % Ar/96 vol % He mixture was used. Argon was introduced to the mixture as an inert tracer. Other mixtures containing 1.3 and 0.7 vol % of N_2O were created by dilution with He in the Micromeritics 2910 analyzer. The same total flow rate was used for all gas compositions (20 mL (STP)/min).

Two methods for the determination of the Fe(II) sites were

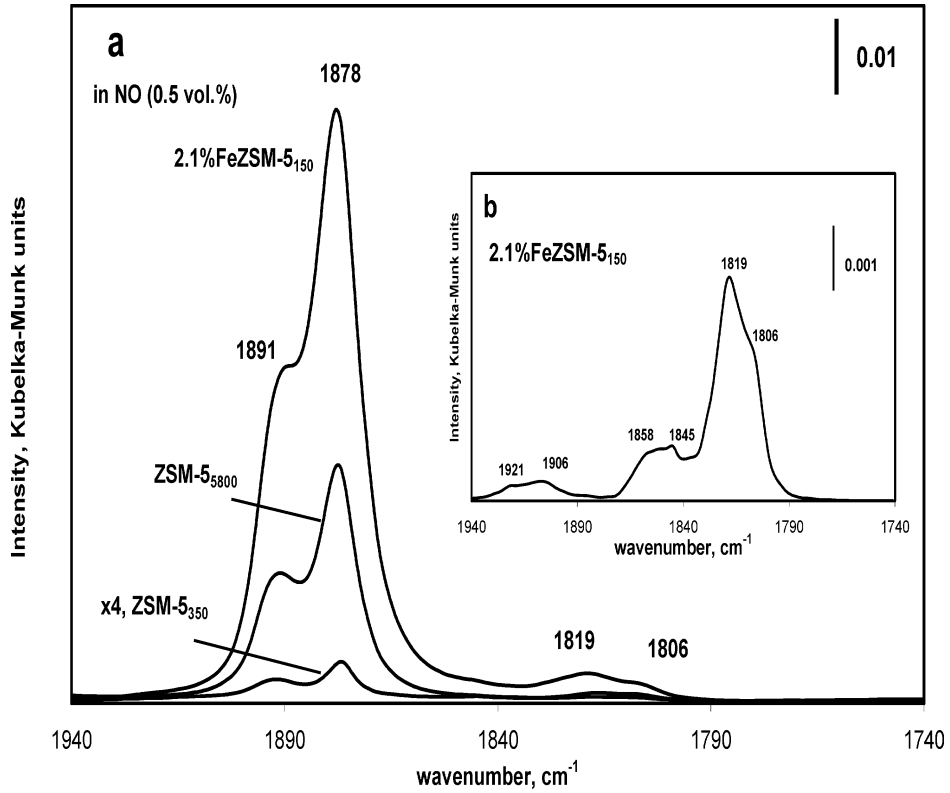

Figure 1. DRIFT spectra at 303 K (a) of nitrosyl region obtained during NO interaction (0.5 vol %, 6 min) with different ZSM-5 catalysts activated in He for 1 h at 1323 K; (b) of nitrosyl species removed from the 2.1%Fe−ZSM-5_{150} catalyst during 3 min of purge by Ar.

applied with a Micromeritics AutoChem 2910 analyzer as described elsewhere.[21] They were based on the total amount of oxygen loaded from N_2O on a zeolite (N_2 formed in reaction 1, C_{Fe}^{Σ} in Table 1) and on the amount of oxygen desorbed at 630−670 K after the N_2O interaction for 5 min (reaction 3, C_{Fe}^{TPD}, Table 1). It was shown earlier[18,21] that these two methods give different amounts of Fe sites: $C_{Fe}^{\Sigma} > C_{Fe}^{TPD}$.

NO interaction with a catalyst was performed for 5 min with a 0.5 vol % NO/0.5 vol % Ar/99 vol % He mixture. After N_2O or NO reacted with the catalyst, the reactor was purged by He for 10 min, and temperature-programmed desorption (TPD) was performed in He (20 mL/min, STP) with a 30 K/min ramp. Gas purities were higher than 99.998%, except for NO, which was >99.9%.

3. Results

3.1. NO Adsorption on the Surface Iron Sites. The iron sites were probed by infrared spectroscopy of adsorbed NO at room temperature. This is a developing method for the iron sites characterization in zeolites,[22−29] which gives some hints concerning their oxidation state, nuclearity, and coordination. The DRIFT spectra presented in Figure 1a were obtained for the catalysts prepared by different methods, such as hydrothermal synthesis and postsynthesis iron deposition (2.1%Fe−ZSM-5) (Table 1). The spectra of the nitrosyl region obtained after 6 min of the NO (0.5 vol %) interaction with zeolites at 303 K in the presence of gaseous NO were similar. They showed two strong bands at 1891 and 1878 cm^{-1} with the same ratio of intensities and weak bands at 1819 and 1806 cm^{-1} (Figure 1a). Only the former species were stable in a flow of Ar at room temperature. The nitrosyl species characterized by the region of 1870−1890 cm^{-1} were found also stable in the presence of 0.5 vol % NO at a temperature as high as 603 K.

The two strong bands at 1870−1890 cm^{-1} were observed earlier for different Fe−ZSM-5 samples.[12,24,25] However, two strong bands at 1856 and 1882 cm^{-1} [23,30] or only one band at around 1880 cm^{-1} were also reported.[3,22,23,31−33] The differences could be due to different NO partial pressures, time-on-stream, temperature, conditions of catalysts synthesis, activation, and pretreatments. The two species giving the bands at 1870−1890 cm^{-1} were reported to possess high, but quite similar thermal stability.[25] In accordance with our data, they were found stable in the presence of 0.5% NO/He at 673 K[31] and in He at 573 K.[24] However different reactivity of these two species with oxygen was reported,[25] indicating different species responsible for two bands.

The catalyst activation and pretreatments used in the present work implied the formation of extraframework iron, its autoreduction to the Fe(II) state, and dehydroxylation.[18,19] It was observed that the intensity of the bands at 1870−1890 cm^{-1} increased after the thermal treatment of hydrothermally synthesized ZSM-5 samples in He at 1323 K as compared to the thermal treatment at 823 K. This suggests that the high-temperature treatment increases the amount of sites responsible for NO adsorption. The band intensities of adsorbed NO (1870−1890 cm^{-1}) increased with the number of active iron sites involved in the surface oxygen loading presented in Table 1 as C_{Fe}^{Σ}. Up to 80% of iron content in the sample ZSM-5_{350} was able to load oxygen, indicating that iron in this sample was mainly in the Fe(II) state before the NO adsorption. Additionally, it is known that the adsorption of NO on Fe(III) sites is much weaker than on Fe(II) sites. Hence, the detected nitrosyl species are assigned to iron in the state Fe(II). In accordance, no band in the region 1870−1890 cm^{-1} was observed for the similarly treated Fe_2O_3 (Fluka, >99%) or $Fe_2(SO_4)_3$·aq (Fluka) dehydrated at 373 or 473 K.

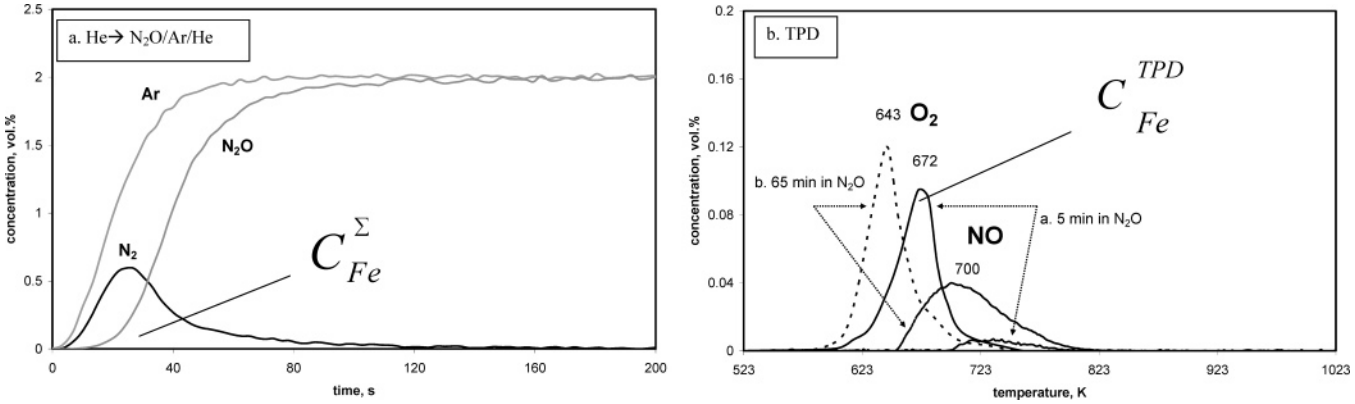

Figure 2. (a) Response curves of N_2 and N_2O obtained at 523 K during introduction of the 2 vol % N_2O, 2 vol % Ar mixture in He on the ZSM-5_{350} catalyst pretreated in He at 1323 K for 1 h. Inert tracer (Ar) response is shown for comparison; (b) TPD profiles of oxygen and NO after 5 (a) and 65 (b) min of the N_2O interaction (2 vol %) with the ZSM-5_{350} catalyst pretreated in He at 1323 K for 1 h.

A discrepancy is in the literature concerning the coordination and nuclearity of the iron sites responsible for the 1870−1890 cm^{-1} region. These sites were assigned to isolated iron sites located in β positions of zeolite;[23,30] however, a detailed analysis showed that oligonuclear species are more probable.[3,25,26,34] These species were also associated with the extraframework Fe species attached to Al cations via bridging oxygen atoms[25] because the bands in this region were not observed for Fe−silicalites without aluminum.[22,25] Hence, the bands in this region we assigned to mononitrosyl $Fe^{2+}(NO)$ species involved in surface bi- and oligonuclear iron species, probably with aluminum in vicinity.

As the species with the bands at 1891 and 1878 cm^{-1} were stable without gaseous NO at room temperature, the unstable species could be distinguished. The spectrum after the subtraction of the stable species bands is very weak (Figure 1b). The bands at 1819, 1806, 1845, 1858, 1921, and 1906 cm^{-1} are seen. The couples of bands in the regions of 1810 and 1915 cm^{-1} were assigned earlier to dinitrosyl $Fe^{2+}(NO)_2$ [24,29,30,34] or trinitrosyl $Fe^{2+}(NO)_3$ [22,26] species. It is evident that the iron species accepting two or three NO molecules should possess high coordinative unsaturation and are probably isolated.[22,26,35] The band at around 1770 cm^{-1}, accompanied[22,35] or not accompanied[29,30] by the 1845 cm^{-1} band assigned earlier to dinitrosyls or mononitrosyls, respectively, was not observed in the present study.

The bands in the range of 1860−1840 cm^{-1} seen on Figure 1b were assigned earlier to mononitrosyls $Fe^{2+}(NO)$[3,23,25,29] associated with isolated iron sites. It should be noted that the band with the close position was observed on Fe−silicalites without aluminum.[25]

From the DRIFTS experiments, it follows that Fe(II) species in the studied zeolites are not uniform. A comparison of the relative band intensities with the literature data[22,29,30,35] shows that the intensity of the bands shown in Figure 1b are extremely weak with respect to the bands of 1878 and 1891 cm^{-1}. Hence, the concentration ratio of the isolated iron species responsible for the bands in Figure 1b to other species present (bi- and oligonuclear, probably with aluminum in vicinity) is small, if not negligible, for the studied samples.

3.2. NO Formation from N_2O. N_2O interaction with different Fe−ZSM-5 catalysts (Table 1) was studied by the transient response method, followed by the TPD in He. It is seen in Figure 2a that, after the N_2O introduction, the N_2O-concentration curve is shifted with respect to the inert tracer (Ar). This shift is due to N_2O reversible adsorption and its transformation to atomic surface oxygen and gaseous N_2.[18] Nitrogen was the only gaseous product observed. No gaseous NO/NO_2 formation was detected by the NO_x detector (≥10 ppm sensitivity). The amount of N_2 evolved was used to estimate the total amount of surface Fe(II) sites involved in oxygen loading (C_{Fe}^{Σ}, Table 1). This assignment is formal: N_2 appears as an asymmetric peak with a tailing up to 200 s. This shape of the N_2 response could not be described by the rate of reaction 1 on a single type of sites. The response pattern suggests also another source of N_2 formation.

After 5 and 65 min of interaction of the gas mixture containing 2 vol % of N_2O with the ZSM-5_{350} catalyst at 523 K and He purge, the TPD runs were performed (Figure 2b). It is seen that adsorbed NO and oxygen loaded during the N_2O interaction could be removed from the surface during the TPD with the peaks at around 700 K for NO and 630−670 K for oxygen. The amount of iron sites able to desorb oxygen (C_{Fe}^{TPD}, Table 1) was lower than the total amount of iron sites involved in the oxygen loading from N_2O (C_{Fe}^{Σ}, Table 1). This indicates that iron sites of a different nature are present. Some of them could accept oxygen from N_2O, but cannot evolve O_2 at 630−670 K in the TPD. Another reason for this difference could be due to N_2 release during the surface NO formation from N_2O:

$$2N_2O_{ads} \rightarrow N_2 + 2NO_{ads} \qquad (4)$$

It is seen from Table 1 that the thermal activation of the same zeolite synthesized by the hydrothermal method at 1323 K provides a higher amount of active sites as compared to the activation by steaming and heating at 823 K. The catalyst prepared by postsynthesis iron deposition (2.1%Fe−ZSM-5_{150}) is almost not sensitive to the activation temperature. The gap between C_{Fe}^{Σ} and C_{Fe}^{TPD} is bigger for these catalysts, indicating that some Fe(II) is present in the form of iron oxide particles, which can load some oxygen from N_2O, but do not desorb it at 630−670 K. Long time activation of the ZSM-5_{5800} catalyst at 1323 K results in a decrease of the amount of active sites, contrary to the catalysts with much lower concentration of iron (ZSM-5_{200}).[18,19] This can be a result of agglomeration of iron to inactive iron oxide particles.

The amount of NO accumulated on the surface increased almost 1 order of magnitude when the interaction time with N_2O increased from 5 to 65 min (Figure 2b). This increase was concomitant with a ∼30 K shift of the oxygen TPD peak to lower temperatures, indicating an easier desorption of oxygen due to NO in agreement with our earlier data.[1] It is important that the amount of O_2 desorbed in the TPD run remained independent of the time of N_2O interaction with the zeolite. The time dependences of the NO amount accumulated on ZSM-

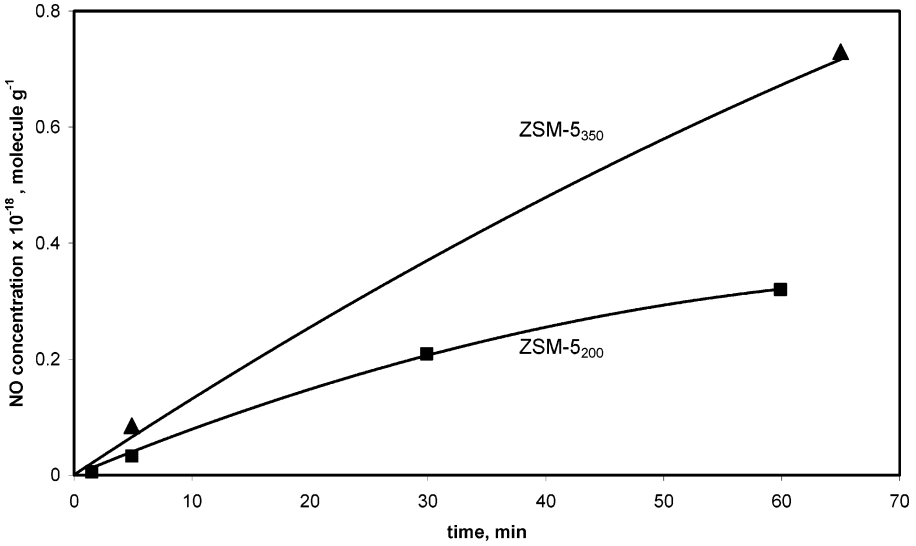

Figure 3. Time dependence of the adsorbed NO accumulation (C_{NO}^{TPD}) from N_2O (2 vol %) at 523 K on the ZSM-5_{350} and ZSM-5_{200} catalysts activated in He at 1323 K.

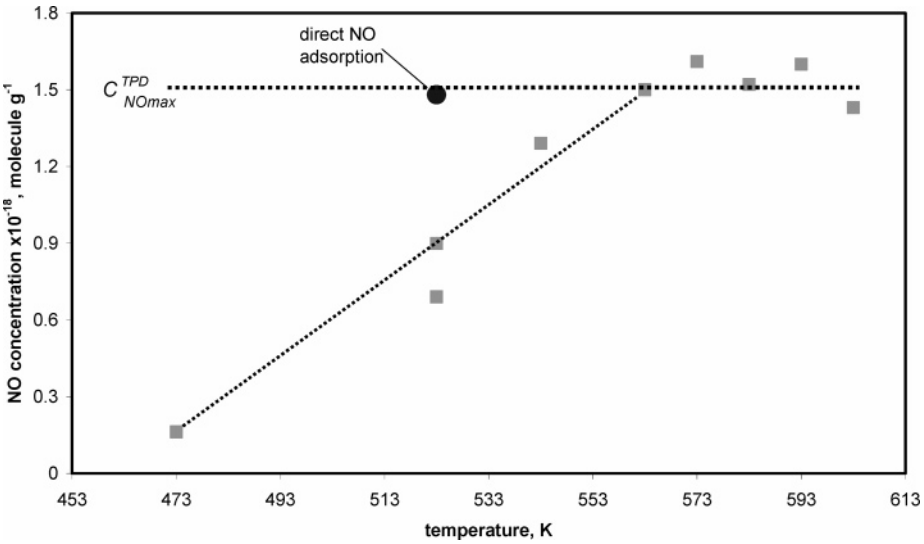

Figure 4. Dependence of the concentration of adsorbed NO species (C_{NO}^{TPD}) accumulated on the ZSM-5_{350} catalyst during 65 min of the interaction with N_2O (2 vol %) on the temperature. A result of direct adsorption of NO (0.5 vol %, 5 min) is shown for comparison.

5_{350} and ZSM-5_{200} catalysts during the interaction with N_2O are shown in Figure 3. The ZSM-5_{350} catalyst possessing a higher amount of active iron sites than the ZSM-5_{200} (Table 1) accumulates more NO formed from N_2O during the same period. This suggests that the sites active in the NO formation are related to iron.

The N_2O interaction with the ZSM-5_{350} catalyst was also performed at different temperatures to determine the amount of the accumulated, adsorbed NO. For this purpose, after 65 min of the reaction at the selected temperature (>523 K), the reactor was quickly cooled in the reaction mixture to 523 K, purged with He for 10 min, and the TPD was performed. The NO amount produced from N_2O and accumulated on the surface was calculated and plotted as a function of temperature (Figure 4). It is seen that the concentration increases, reaching a maximum value equal to 1.5×10^{18} molecules g^{-1}, which does not change in the range 563−603 K. The maximum value may correspond to the saturation of the sites, which adsorb NO irreversibly because desorption of NO starts only at higher temperatures (>653 K). The NO adsorption was also performed directly from gas phase on the ZSM-5_{350} catalyst to obtain a maximal amount of the sites. For this purpose, a mixture containing 0.5 vol % of NO was contacted with the catalyst for 5 min at 523 K, and after He purge, the TPD was performed. The amount of NO desorbed was equal to the amount of NO produced from N_2O at temperatures 563−603 K. This value was 2 times higher than the concentration of adsorbed NO formed from N_2O at 523 K for 65 min (Figure 4). These data indicate that the maximal concentration of sites, which adsorbed NO is equal to 1.5×10^{18} sites g^{-1}, and that, after 65 min at 523 K, the produced NO from N_2O was not sufficient to cover all sites. The maximum number of NO sites (C_{NOmax}^{TPD}) was taken for kinetic modeling of N_2O decomposition in our previous publication.[17] This value corresponds to ∼75% of the active Fe(II) sites determined by the TPD ($C_{Fe}^{TPD} = 2.0 \times 10^{18}$ sites g^{-1}).

Figure 5 shows the effect of the initial N_2O concentration on the NO formation. In these experiments, the catalyst was contacted with the reaction mixture containing different concentrations of N_2O (2, 1.3, and 0.7 vol %) at 523 K for 5 min, and then heated in the reaction mixture at 10 K/min. It is seen

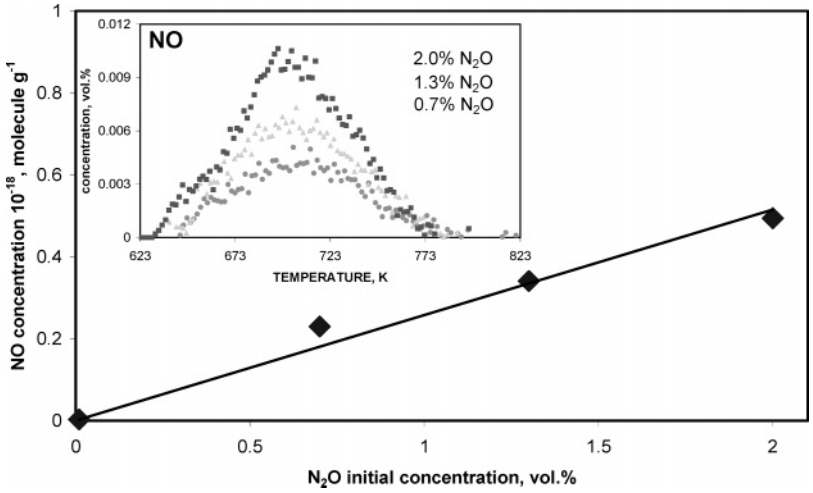

Figure 5. Dependence of the concentration of the evolved NO on the initial concentration of N_2O in gas mixture determined after 5 min of the N_2O interaction with the ZSM-5_{350} catalyst activated in He at 1323 K followed by the temperature programmed reaction (TPR). Inset: NO profiles during TPR: squares, 2 vol % N_2O; triangles, 1.3 vol % N_2O; circles, 0.7 vol % N_2O.

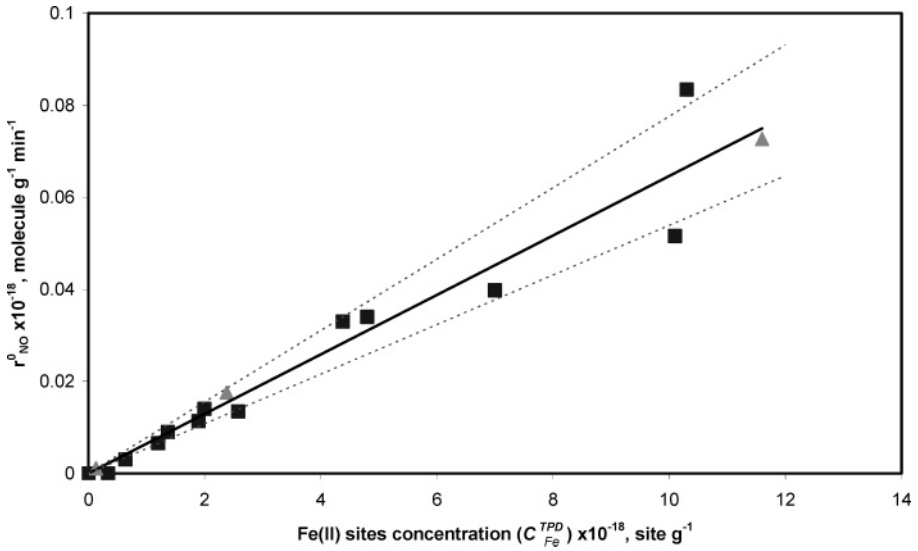

Figure 6. Dependence of the initial rate of the adsorbed NO species formation on the surface of different Fe−ZSM-5 catalysts (Table 1, squares, activated at 1323 K; triangles, activated at 823 K) from N_2O (2 vol %) during 5 min at 523 K on the concentration of the sites evolving oxygen from these catalysts at 630−670 K (C_{Fe}^{TPD} from the TPD data).

that NO evolved in different amounts (Figure 5, inset). The higher the concentration of N_2O, the higher the amount of the evolved NO. Roughly linear first-order dependence is observed for the NO formation on the concentration of N_2O, as shown in Figure 5.

3.3. Rate of NO Formation from N_2O. The N_2O interaction with different ZSM-5 catalysts (Table 1) was performed for 5 min at 523 K, and the amounts of adsorbed NO and loaded oxygen from N_2O were determined from the TPD profiles (Figure 2b). As the adsorption of NO is irreversible and is far from saturation of adsorption sites, the amount of adsorbed NO during 5 min of reaction of N_2O is proportional to the initial rate of its formation from N_2O. Thus, the rates were calculated for the samples with different concentrations of the active Fe(II) sites (Table 1).

A correlation of NO formation was found between the rate and the concentration of the sites evolving oxygen during the TPD at 630−670 K (C_{Fe}^{TPD}) and is presented in Figure 6. Neither oxygen nor NO were observed in the TPD after the N_2O interaction with the Fe_2O_3/Al_2O_3 catalyst (0.20 g, Fe 5 wt %) pretreated in the same way as the Fe−ZSM-5 samples. Thus, iron oxide particles were not responsible for the NO formation/accumulation. On the contrary, the amount of adsorbed NO increased with the amount of Fe sites evolving oxygen at 630−670 K. It is interesting that the temperature of the zeolite activation (823 or 1323 K) had no effect on the observed dependence (Figure 6, triangles and squares), showing that the same sites were formed after both activations. The straight line indicates that the formation/accumulation of NO takes place either with participation of the sites responsible for oxygen desorption or on the sites related to them. The latter seems more probable, as for the ZSM-5_{350} sample, the maximum coverage by NO equals only 75% from C_{Fe}^{TPD}. Additionally, as is seen from Figure 2b, the adsorbed NO does not block the sites for the oxygen loading from N_2O, as the concentration of oxygen in the TPD peak does not decrease when the NO concentration increases considerably. This conclusion corresponds to the reported data[1,11] on the effect of NO in N_2O decomposition to O_2 and N_2, confirming noncompetitive adsorption.

4. Discussion

Adsorbed NO was found to be formed from N_2O during its interaction with Fe-containing ZSM-5 catalysts at low temper-

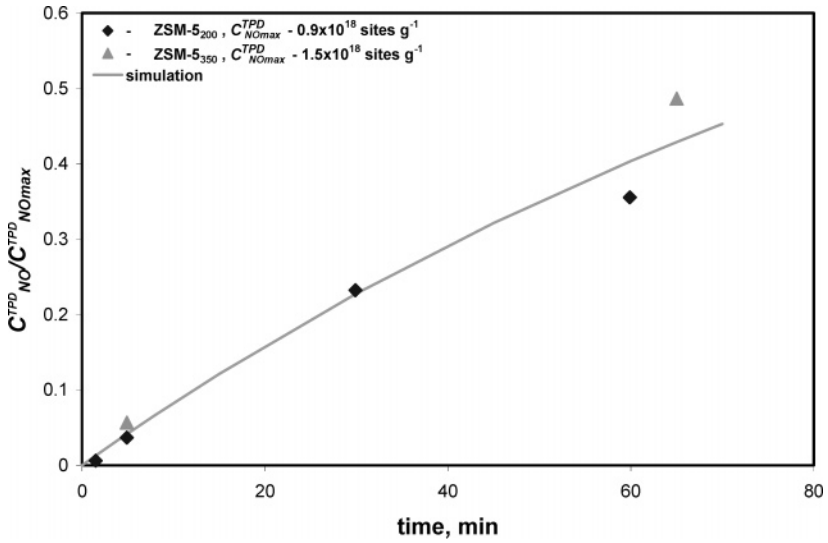

Figure 7. The dynamics (simulated and measured) of adsorbed NO formation from N_2O (2 vol %, 523 K) related to the maximal NO coverage on the ZSM-5_{350} and ZSM-5_{200} catalysts activated in He at 1323 K.

atures (473−603 K). The accumulated amounts of NO do not correspond to an impurity in N_2O: in order to accumulate the determined amounts of NO (3.5×10^{17} NO molecules g^{-1}) during 5 min of the N_2O reaction with the samples with high iron content, N_2O should contain up to 0.5% of NO_x. This concentration could be easily monitored by the NO/NO_x detector, but it was not the case. This is also in line with the observed dependence of the adsorbed NO concentration on the temperature (Figure 4). Additional evidence that NO is not present as an impurity in N_2O was obtained by the comparison of the oxygen dynamics curves at different temperatures,[17] which were found to be dependent on the temperature. The increase of the reaction rate was more marked for higher temperatures, confirming the chemical interaction of N_2O with the surface leading to adsorbed NO, but not accumulation of NO impurity.

The amount of active iron sites, on which NO accumulation takes place, is generally low and does not exceed $3 \cdot 10^{19}$ sites g^{-1} (Table 1).[21] A slow increase of the adsorbed NO concentration takes place during more than 1 h of the N_2O interaction with zeolite at 523 K (Figure 3). These species desorb at temperatures higher than 643 K (Figure 2b). The formation of NO species in the Fe−ZSM-5 samples was proportional to the N_2O concentration (Figure 5). Hence, the adsorbed NO species is quite difficult to detect during or after the N_2O decomposition performed over the Fe−ZSM-5 catalysts with low iron content, at low N_2O pressures, low time-on-streams, or temperatures higher than 643 K.

DRIFTS of adsorbed NO at room temperature (Figure 1a) shows heterogeneity of iron sites. Adsorbed NO was mainly presented by the species characterized by the bands at around 1870−1890 cm^{-1} (Figure 1a). These species possessed high thermal stability, indicating strong interaction of NO with iron. Assignment of these bands to Fe(II) involved in bi- and oligonuclear sites associated with aluminum extraframework cations seems possible; however, this point requires further studies. The contribution of the sites with high coordinative unsaturation (probably isolated) is low.

Insight concerning the sites involved in NO formation by measuring the NO amount formed from N_2O on activated ZSM-5 catalysts with different acidity, amount of iron, and concentration of active iron species (Table 1) was also obtained. It was demonstrated that there is a relationship between the iron sites, which form oxygen from N_2O desorbing at 630−670 K and the sites, which may form adsorbed NO from N_2O (Figure 6). Desorption of oxygen from isolated iron sites is more difficult than that from bi and and oligonuclear iron sites. Diffusion of one oxygen atom to another over the ZSM-5 surface is necessary in this case. Hence, the iron sites evolving oxygen at 630−670 K were assigned to bi- and/or oligonuclear ones.[18,21] Thus, the initial rate of the adsorbed NO formation is proportional to the N_2O concentration (C_{N_2O}) and concentration of the iron sites evolving oxygen C_{Fe}^{TPD}:

$$r^0_{NO} \sim C_{N_2O}\, C_{Fe}^{TPD} \tag{5}$$

Nitrogen evolution during the N_2O interaction accompanied by oxygen loading is finished within ~2 min (Figure 2), but the accumulation of the strongly adsorbed NO species was slow and was observed for more than 60 min (Figure 3). Hence, the step of N_2O decomposition to surface atomic oxygen and gaseous nitrogen is much faster than the accumulation of surface NO species and the oxidized iron sites $(O)_{Fe}$ could participate in the formation of adsorbed NO.

A simplified kinetic scheme of the N_2O interaction with Fe−ZSM-5 at low temperatures (≤563 K) can be presented as:

$$N_2O_{gas} \leftrightarrow N_2O_{ad}$$
(reversible adsorption) instantaneous (6)

$$N_2O_{ad} + (\ )_{Fe} \rightarrow N_2 + (O)_{Fe}$$
(deposition of oxygen) fast (7)

$$N_2O_{ad} + (O)_{Fe} \rightarrow 2[NO]' + (\ )_{Fe}$$
(formation of surface NO) relatively fast (8)

$$[NO]' \rightarrow [NO]$$
(accumulation of catalytic NO) slow (9)

Step 6 corresponds to reversible adsorption of N_2O, followed by the surface atomic oxygen loading, accompanied by N_2 evolution (step 7). The adsorbed NO, [NO]′, is formed in step 8, followed by the reaction 7 with participation of the liberated $(\ )_{Fe}$ sites, additionally giving N_2 in the gas phase. Evidence for the relatively fast step 8 could come from the pattern of the N_2 response. During the N_2O interaction, nitrogen appears as an asymmetric peak with a tail up to 200 s. This shape of the N_2 response could not be described by only the rate constant of

the reaction 7. The response pattern suggests also another source of the N_2 formation and was proposed via reactions 8 and 7 together.[17] Another reason for the tailing of the N_2 peak may come from the heterogeneity of the iron sites (DRIFTS) involved in the oxygen loading on the surface presented by reaction 7. Because the accumulation of NO at temperatures $T \leq 600$ K is a slow process (Figure 3), a slow transformation of the [NO]′ species to the [NO] species was suggested and described by the step 9.

The transformation of the adsorbed NO to adsorbed NO_2 species via the oxidation by the loaded oxygen can also take place.[2,4,12,17] All of these factors are difficult to take into account for simulation of the adsorbed NO accumulation in time (Figure 3). It is important that a satisfactory description of the dynamics of the accumulation was obtained for two samples (Figure 7) by using a simple equation:

$$C_{NO}^{TPD}/C_{NOmax}^{TPD} = 1 - \exp(-kt) \quad (10)$$

implying that the slowest step of the NO adsorption/formation takes place on unoccupied sites. In this equation, t is the time-on-stream, and k represents the initial rate of the adsorbed NO formation related to the maximal concentration of the sites, which can adsorb NO (C_{NOmax}^{TPD}):

$$k = r^0_{NO}/C_{NOmax}^{TPD} \quad (11)$$

where C_{NOmax}^{TPD} was assumed to be 75% from the amount of the sites that evolved oxygen at 630−670 K, C_{Fe}^{TPD}, and was 1.5×10^{18} sites g^{-1} for the ZSM-5_{350} and 0.9×10^{18} sites g^{-1} for the ZSM-5_{200} sample. The k value was determined from Figure 6 and related to 75% of the C_{Fe}^{TPD}, being equal to 0.0049 min^{-1}.

In our previous publications[1,17] a considerable increase of the N_2O decomposition rate in time until reaching a steady state at 563−603 K was shown and assigned to the accumulation of surface NO species catalyzing the reaction. This was in accordance with the adsorbed NO formation dynamics (Figures 3, 7). Direct introduction of the NO pulse into the N_2O mixture reacting with the ZSM-5_{200} catalyst at 603 K provided an immediate reaching of a steady state.[1] Thus, the observed rate increase was assigned to autocatalysis by NO. The adsorbed NO could lead to an increase of the N_2O decomposition rate via a promotion of the oxygen desorption (reaction 3a), which is the rate-determining step. This step is not elementary and will be considered in detail in a forthcoming publication.

5. Conclusions

DRIFTS of adsorbed NO as a probe molecule at room temperature indicated different Fe(II) sites with a roughly similar ratio of concentrations in the studied zeolites. Adsorbed NO formation from N_2O was found to take place on Fe−ZSM-5 catalysts at 473−603 K. The initial rate of the NO formation at 523 K was observed to be first order in N_2O partial pressure and was linearly dependent on the concentration of active bi- and oligonuclear Fe(II) sites. The amount of these sites, C_{Fe}^{TPD}, was determined by desorbing oxygen at 630−670 K after Fe(II) loading by atomic oxygen from N_2O at 523 K. Adsorbed NO species could be desorbed at around 700 K. The simulated dynamics of adsorbed NO formation from N_2O was consistent with the experimental data.

Acknowledgment. We thank the Swiss Science Foundation for the financial support. The work of Dr. I. Yuranov and A. Udriot for synthesis of some catalysts and Fe content determination is highly appreciated.

Note Added after ASAP Publication. This article was published ASAP on December 8, 2005. The citation of ref 16 was changed to a citation of ref 17 in the paragraph following eq 9. The correct version was reposted on December 12, 2005.

References and Notes

(1) Bulushev, D. A.; Kiwi-Minsker, L.; Renken, A. *J. Catal.* **2004**, *222*, 389.
(2) El-Malki, E. M.; van Santen, R. A.; Sachtler, W. M. H. *J. Catal.* **2000**, *196*, 212.
(3) Grubert, G.; Hudson, M. J.; Joyner, R. W.; Stockenhuber, M. *J. Catal.* **2000**, *196*, 126.
(4) El-Malki, E. M.; van Santen, R. A.; Sachtler, W. M. H. *Microporous Mesoporous Mater.* **2000**, *35*−*6*, 235.
(5) Mauvezin, M.; Delahay, G.; Coq, B.; Kieger, S.; Jumas, J. C.; Olivier-Fourcade, J. *J. Phys. Chem. B* **2001**, *105*, 928.
(6) Novakova, J.; Schwarze, M.; Sobalik, Z. *Catal. Lett.* **2005**, *104*, 157.
(7) Shimokawabe, M.; Hirano, K.; Takezawa, N. *Catal. Today* **1998**, *45*, 117.
(8) Turek, T. *Appl. Catal., B* **1996**, *9*, 201.
(9) Kapteijn, F.; Marban, G.; Rodriguez-Mirasol, J.; Moulijn, J. A. *J. Catal.* **1997**, *167*, 256.
(10) Perez-Ramirez, J.; Kapteijn, F.; Mul, G.; Xu, X. D.; Moulijn, J. A. *Catal. Today* **2002**, *76*, 55.
(11) Perez-Ramirez, J.; Kapteijn, F.; Mul, G.; Moulijn, J. A. *J. Catal.* **2002**, *208*, 211.
(12) Mul, G.; Perez-Ramirez, J.; Kapteijn, F.; Moulijn, J. A. *Catal. Lett.* **2001**, *77*, 7.
(13) Sang, C. M.; Lund, C. R. F. *Catal. Lett.* **2001**, *73*, 73.
(14) Kogel, M.; Abu-Zied, B. M.; Schwefer, M.; Turek, T. *Catal. Commun.* **2001**, *2*, 273.
(15) Boutarbouch, M. N. D.; Cortes, J. M. G.; El Begrani, M. S.; de Lecea, C. S. M.; Perez-Ramirez, J. *Appl. Catal., B* **2004**, *54*, 115.
(16) Sang, C. M.; Kim, B. H.; Lund, C. R. F. *J. Phys. Chem. B* **2005**, *109*, 2295.
(17) Kiwi-Minsker, L.; Bulushev, D. A.; Renken, A. *Catal. Today* **2005**, *110*, 191.
(18) Kiwi-Minsker, L.; Bulushev, D. A.; Renken, A. *J. Catal.* **2003**, *219*, 273.
(19) Kiwi-Minsker, L.; Bulushev, D. A.; Renken, A. *Catal. Today* **2004**, *91*−*92*, 165.
(20) Bulushev, D. A.; Kiwi-Minsker, L.; Renken, A. *Catal. Today* **2000**, *57*, 231.
(21) Yuranov, I.; Bulushev, D. A.; Renken, A.; Kiwi-Minsker, L. *J. Catal.* **2004**, *227*, 138.
(22) Berlier, G.; Zecchina, A.; Spoto, G.; Ricchiardi, G.; Bordiga, S.; Lamberti, C. *J. Catal.* **2003**, *215*, 264.
(23) Lobree, L. J.; Hwang, I.-C.; Reimer, J. A.; Bell, A. G. *J. Catal.* **1999**, *186*, 242.
(24) Lezcano, M.; Kovalchuk, V. I.; d'Itri, J. L. *Kinet. Katal.* **2001**, *42*, 104.
(25) Mul, G.; Perez-Ramirez, J.; Kapteijn, F.; Moulijn, J. A. *Catal. Lett.* **2002**, *80*, 129.
(26) Nechita, M. T.; Berlier, G.; Ricchiardi, G.; Bordiga, S.; Zecchina, A. *Catal. Lett.* **2005**, *103*, 33.
(27) Joyner, R.; Stockenhuber, M. *J. Phys. Chem. B* **1999**, *103*, 5963.
(28) Hensen, E. J. M.; Zhu, Q.; van Santen, R. A. *J. Catal.* **2005**, *233*, 136.
(29) Chen, H. Y.; El-Malki, E. M.; Wang, X.; van Santen, R. A.; Sachtler, W. M. H. *J. Mol. Catal. A* **2000**, *162*, 159.
(30) Lobree, L. J.; Hwang, I. C.; Reimer, J. A.; Bell, A. T. *Catal. Lett.* **1999**, *63*, 233.
(31) Sun, Q.; Gao, Z. X.; Chen, H. Y.; Sachtler, W. M. H. *J. Catal.* **2001**, *201*, 89.
(32) Gao, Z. X.; Qi, S.; Sachtler, W. M. H. *Appl. Catal., B* **2001**, *33*, 9.
(33) Hadjiivanov, K.; Knozinger, H.; Tsyntsarski, B.; Dimitrov, L. *Catal. Lett.* **1999**, *62*, 35.
(34) Mul, G.; Zandbergen, M. W.; Kapteijn, F.; Moulijn, J. A.; Perez-Ramirez, J. *Catal. Lett.* **2004**, *93*, 113.
(35) Berlier, G.; Ricchiardi, G.; Bordiga, S.; Zecchina, A. *J. Catal.* **2005**, *229*, 132.